ISOLATING CLUSTERS WITH WOLF-RAYET STARS IN I ZW 18[1]

THOMAS M. BROWN
Space Telescope Science Institute, 3700 San Martin Drive, Baltimore, MD 21218. tbrown@stsci.edu
SARA R. HEAP, IVAN HUBENY, THIERRY LANZ, DON LINDLER
Code 681, NASA Goddard Space Flight Center, Greenbelt, MD 20771. heap@srh.gsfc.nasa.gov, hubeny@tlusty.gsfc.nasa.gov, lanz@nova.gsfc.nasa.gov, lindler@rockit.gsfc.nasa.gov

To appear in The Astrophysical Journal Letters

ABSTRACT

We present UV images and spectra of the starburst galaxy I Zw 18, taken with the Space Telescope Imaging Spectrograph. The high spatial resolution of these data allows us to isolate clusters containing Wolf-Rayet stars of the subtype WC. Our far-UV spectra clearly show C IV $\lambda\lambda$1548,1551 and He II λ1640 emission of WC stars in two clusters: one within the bright (NW) half of I Zw 18, and one on the outskirts of this region. The latter spectrum is unusual, because the C IV is seen only in emission, indicating a spectrum dominated by WC stars. These data also demonstrate that the H I column in I Zw 18 is strongly peaked in the fainter (SE) half of I Zw 18, with a column depth far larger than that reported in previous analyses.

Subject headings: stars: Wolf-Rayet – galaxies: starburst – galaxies: stellar content – ultraviolet: galaxies

1. INTRODUCTION

I Zw 18 (Mrk 116) represents an important local fiducial in our understanding of galaxy formation and evolution. It is a blue compact galaxy with the smallest known abundance of heavy elements in its ionized gas ($\sim$2% of solar; Vílchez & Isglesias-Páramo 1998 and references therein). For the past three decades, debate since has focused on the age of its stellar populations. Early analyses of Wide Field Planetary Camera 2 (WFPC2) images suggested that star formation began several tens of Myr ago (Dufour et al. 1996; Hunter & Thronson 1995), while later analyses of the same WFPC2 images (Aloisi, Tosi, & Greggio et al. 1999) and new images from the Near Infrared Camera and Multiobject Spectrometer (Östlin 2000) implied the presence of an older population (0.5–1 Gyr) from a small number of faint red stars.

Two independent sets of ground-based observations have recently discovered Wolf-Rayet (WR) emission within the brighter (NW) component of I Zw 18: Izotov et al. (1997) found evidence for 17 WN and 5 WC stars, while Legrand et al. (1997) found evidence for 1–2 WC stars. While neither group had the spatial information to tie this emission to stellar clusters, the existence of WR stars in I Zw 18, especially of subtype WC, is surprising, because canonical (non-rotating and non-binary) evolutionary theory predicts few WN stars and no WC stars to form at the low metallicity of I Zw 18 (Cerviño & Mas-Hesse 1994; Meynet 1995). de Mello et al. (1998) subsequently searched for these WR stars in narrow-band WFPC2 images, and found faint peaks in the He II λ4686 emission they attributed to either nebular emission or 5–9 WN stars.

Using the Space Telescope Imaging Spectrograph (STIS) on board the Hubble Space Telescope (HST), we recently obtained a two-dimensional far-UV spectroscopic map of I Zw 18, along with far-UV and near-UV images, in order to further understand its star-formation history. These data reveal two clusters containing WC stars. While neither of these clusters is associated with the WR detections of Legrand et al. (1997) and de Mello et al. (1998), one of the clusters might be responsible for the WC emission seen by Izotov et al. (1997). Our STIS data also provide a high-resolution H I map, based on the Ly-α absorption; we show that the H I column depth (N_{HI}) is sharply peaked within the SE component.

2. OBSERVATIONS

We obtained far-UV spectra of I Zw 18 from 2002 Feb 9 to 2002 Feb 12, using the G140L grating and the $52'' \times 0.5''$ slit on STIS (for a full description of the instrument, see Woodgate et al. 1998 and Kimble et al. 1998). The field-of-view of the STIS UV detectors is $25'' \times 25''$. We placed the slit at seven adjacent positions in I Zw 18, parallel to the axis of the main body (position angle = 145°), resulting in spatially resolved spectra of its bright star-forming regions (Figure 1). The exposure time at four positions was 6058 s (the central 3 positions and the SW extreme), while at the remaining three positions it was 5376 s. At each slit position, half the exposures were offset from the others by $0.5''$ (20 pixels) along the slit, in order to allow masking of bad, hot, and shadowed pixels in the coaddition, and to smooth over variations in the detector response. The spectra were processed through the standard calibration pipeline, except that we also subtracted an appropriately scaled profile of the dark rate, from a sum of 500 ks of dark exposures. The subtraction of this dark "glow" (which peaks in the upper left-hand quadrant and can be 20 times higher than the nominal 7×10^{-6} cts s^{-1} pix^{-1} dark rate) is important when studying faint extended sources. Finally, we subtracted the airglow spectrum using a region in each spectral image free from source flux.

On 2002 Feb 25, we also obtained far-UV and near-UV images of I Zw 18 using the F25SRF2 and F25QTZ filters, respectively, with bandpasses centered at 1457 Å and 2365 Å, and exposure times of 5331 s and 5786 s. We again used $0.5''$ offsets to allow masking of pixels and smoothing of detector response. All of the frames for each camera were coadded, rescaled, and shifted with the DRIZZLE package in IRAF, in order to match

[1]Based on observations made with the NASA/ESA Hubble Space Telescope, obtained at the Space Telescope Science Institute, which is operated by the Association of Universities for Research in Astronomy, Inc., under NASA contract NAS 5-26555. These observations are associated with proposal 9054.

the G140L spectral images described above.

In addition to our STIS data, we also obtained archival WFPC2 images at longer wavelengths, in the F555W (*V*), F439W (*B*), F336W, and F469N (He II λ4686) filters, for comparison with earlier work. The WFPC2 data were cleaned of cosmic rays, coadded, and drizzled to register with the STIS data. Figure 1 shows a false color image produced from our STIS data in the blue and green channels, and the WFPC2/F555W data in the red channel.

3. ANALYSIS

3.1. *WC Stars*

The CALSTIS pipeline software produces two-dimensional rectified spectral images that are useful for examining the spectral energy distributions (SEDs) of extended objects. These images are linear in wavelength along the x-axis, and linear in spatial extent along the y-axis. Upon examination of these images, we saw a compact source with obvious WR/WC emission

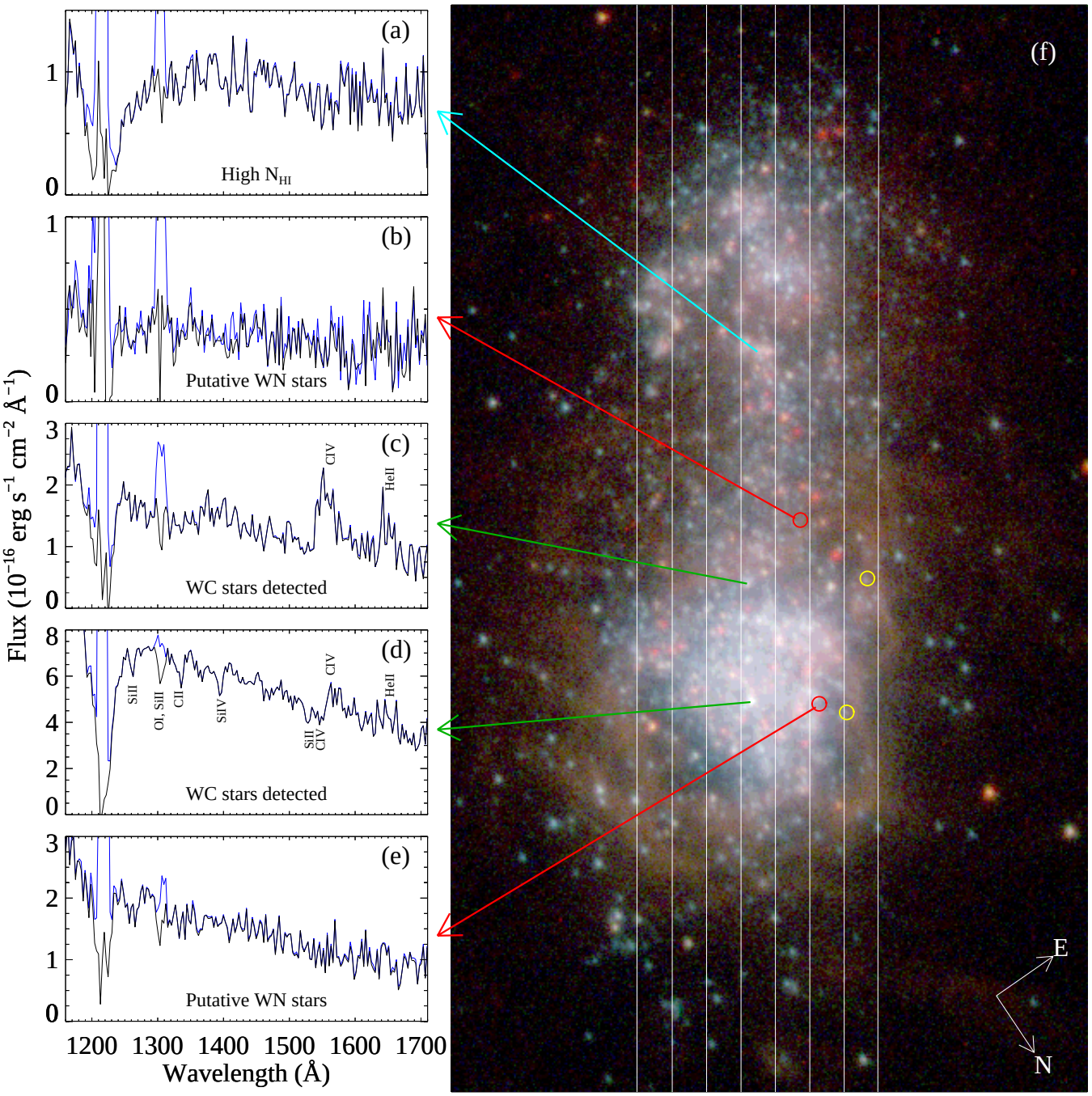

FIG. 1– Far-UV spectra and broad-band images of I Zw 18. Panel a: The spectrum with the broadest Ly-α absorption and thus the highest N_{HI}, with (black) and without (blue) airglow subtraction. Panels b and e: Spectra of regions with previously reported WN detections (de Mello et al. 1998); we find no evidence for WN stars. Panels c and d: Spectra of clusters with WC stars; note the C IV and He II emission lines. Panel f: Composite HST image of I Zw 18 in 3 bandpasses (blue = STIS/FUV/F25SRF2, green = STIS/NUV/F25QTZ, red = WFPC2/F555W). The seven adjacent positions of the STIS slit are marked (white lines). Many of the old stars reported by Aloisi et al. (1999) appear as faint red stars here, but some are UV-bright, indicating a hotter temperature or a hot companion. Yellow circles mark two regions where we find possible narrow He II emission but no associated C IV emission. The deMello et al. (1998) WN detections are encircled in red.

features at C IV $\lambda\lambda$1548, 1551 and He II λ1640 (shown in Figure 1*c*). We then performed a systematic search for other such objects in the data.

To find the locations of individual spectra in these images, we collapsed the spectra along the dispersion axis and convolved with a Gaussian normalized to unit area and zero sum (similar to the finding algorithm of the DAOPHOT package; Stetson 1987). The local maxima in these convolutions gave the y-positions of compact sources along the slit. Returning to the original spectral images, we extracted spectra at each of these positions, using row sums 5 pixels high. We also extracted spectra from the two regions with significant WR/WN detections in previous analyses of WFPC2 data (de Mello et al. 1998; those not marked with "?" in their Table 3), although these regions are not associated with compact sources in our spectral images, or with sources in the UV and optical HST images (compare their Figures 2 and 3*a*). Each spectrum was then shifted to account for the position of the object within the slit, using a centroid on the corresponding region in the far-UV image.

After extracting 205 spectra at the local maxima in our spectral images, we performed a systematic search for broad He II λ1640 emission, using as a guide the spectrum of the source with obvious WR/WC features discussed above. We fit a linear continuum to each spectrum, using spectral regions free of strong emission and absorption features (1400–1500 Å, 1590–1620 Å, and 1670–1710 Å), summed the net flux exceeding this continuum in the region 1635–1665 Å (the heliocentric velocity of I Zw 18 is 751 km s^{-1}; Thuan et al. 1999), and returned a list of $> 3\sigma$ detections of excess flux near 1640 Å. The automated search detected the obvious source we had already found by eye, plus one additional source of WR emission; both spectra also show broad C IV emission, indicating the presence of WC stars (Figure 1, panels *c* and *d*). Note that the emission lines are much broader than a resolution element in our spectra (~ 1 Å for point sources and ~ 12 Å for sources filling the slit). We also found two spectra with narrow emission features near 1640 Å that could be noise or nebular emission; the spectra do not have C IV emission, and their associated clusters are marked in Figure 1*f* (yellow circles).

Our WC detections are located $\sim 1.3''$ SE and $\sim 0.5''$ W of the center of the NW starforming region. Legrand et al. (1997) report WC emission $\sim 1.5''$ SW of the central cluster, so our detections are distinct. Izotov et al. (1997) only restrict their detections of WR stars to the NW starforming region. None of the detections of WN stars by de Mello et al. (1998) correspond to the positions of our WC stars; in Figure 1*b* and 1*e*, we show spectra from the regions of their putative detections.

To estimate the number of WR/WC stars needed to produce the observed He II emission, we used the tabulations of Schaerer & Vacca (1998). In the middle of the range of WC stars, WC5 stars produce an average of He II luminosity of 5×10^{36} erg s^{-1}. Assuming a distance of 12.6 Mpc (Östlin 2000) and a foreground extinction of $E(B-V) = 0.03$ mag (Schlegel, Finkbeiner, & Davis 1998) but no reddening from the patchy internal dust (Cannon et al. 2002), we can convert our He II fluxes to luminosity. For the spectra shown in Figure 1*c* and 1*d*, we measure $L_{1640} = 2.4 \pm 0.5 \times 10^{37}$ erg s^{-1} and $L_{1640} = 3.2 \pm 1.0 \times 10^{37}$ erg s^{-1}, respectively, corresponding to 5$\pm$1 and 6$\pm$2 WR/WC stars. Using the 1500 Å continuum flux and a 5 Myr isochrone (Bertelli et al. 1994), we estimate that these clusters contain 26 and 119 stars, respectively, with with $M > 8\ M_\odot$, suggesting that the ratio WR/(WR+O) in these clusters is respectively 0.2 and 0.05. The stronger WR/WC detection in Figure 1*c* is due to the higher fraction of WR/WC stars in that cluster; note the prominent C IV and Si IV absorption in Figure 1*d*, where the hot underlying population of O stars is more dominant. Our measured WR/(WR+O) ratios fall within the range observed in other galaxies, but are unusually high given the metallicity of I Zw 18 (see Maeder & Meynet 1994). Of course, the ratio is far lower for the galaxy as a whole, given the many UV-bright clusters showing no WR emission.

The ratio of C IV to He II emission in Figure 1*c* is $\sim$2.3, which is typical for the WC subtype (Niedzielski & Rochowicz 1994; Gräfener, Koesterke, & Hamann 2002). However, this ratio is only ~ 0.7 in Figure 1*d*; the smaller ratio is partly due to the C IV absorption from the hot stellar population and interstellar medium, but it could also indicate that one or two of the WR stars in this cluster are of type WN instead of WC.

de Mello et al. (1998) claimed detections of 1.5 and 3 WNL stars, respectively, where we are showing the spectra in Figure 1*b* and 1*e*. Assuming $L_{1640} = 1.6 \times 10^{36}$ erg s^{-1} (Schaerer & Vacca 1996), individual WNL stars would be difficult to detect in our data, but we do not see any signs of these stars. Where de Mello et al. (1998) found 1.5 WNL and 3 WNL stars, we formally find -0.5 ± 3 WNL stars and $+0.5 \pm 1.6$ WNL stars, respectively. Note that there are no point sources in our UV images (or in the extant WFPC2 images) at the locations of the de Mello et al. detections, and de Mello et al. note that their detections are consistent with both nebular or WR emission. Unfortunately, their F469N image has a hot pixel exactly where we have our strongest detection of WR/WC emission, which probably precluded their detection of these sources.

3.2. *Old Clusters or Large Interstellar Hydrogen Column?*

Compared to the spectra in the NW half of I Zw 18, our spectra in the SE half generally show broader Ly-α λ1216 absorption, but it is especially broad in one particular spectrum (see Figure 1*a*). Without other data, the absorption could arise from two situations: either a high column density of interstellar H I, or a predominately older ($\gtrsim$ 500 Myr) and cooler population of stars. We investigated this latter possibility by examining the SED with a longer wavelength baseline than that available in our far-UV spectra. Note that if the spectrum in Figure 1*a* came from a 500 Myr population, it would be have to be $\sim$60 times more massive than the cluster shown Figure 1*d*.

Using the HST images in the far-UV, near-UV, *B*, and *V* bands, we measured the flux in the region of our spectral extraction (an area $0.5'' \times 0.12''$). This flux comes from a string of compact sources aligned with the long axis of the extraction box, so we estimated the aperture correction required by using TinyTim models of the HST PSF in the different bandpasses. We do not expect perfect agreement with the G140L spectrum (due to wavelength-dependent aperture correction uncertainties in the images and spectrum), but they agree at the $\sim$ 10% level (see Figure 2). Furthermore, it is difficult to quantify exactly the dominant effective temperature of the stellar population, given the reddening uncertainties and the fact that we are looking in the Rayleigh-Jeans tail. However, the SED of this region is clearly dominated by a population of hot stars. We show this by integrating the synthetic spectra of Kurucz (1993) over the isochrones of Bertelli et al. (1994), for two different ages (Figure 2). A population of about 500 Myr (or a single star of $T_{\rm eff} \approx 12{,}000$ K) is needed to explain the width of Ly-α absorption without a significant contribution from in-

terstellar H I. However, such a population would produce far more flux at longer wavelengths than is actually seen. Instead, a much younger population (e.g., 16 Myr) reddened by $E(B-V) = 0.06$ mag (SMC extinction law; Witt & Gordon 2000) can reproduce the spectral energy distribution from the far-UV to the optical, but this requires that the Ly-α absorption come from a high H I column: $N_{HI} \approx 2 \times 10^{22}$ atoms cm^{-2}. This result is independent of the dominant T_{eff} in the underlying population, for $T_{eff} \gtrsim 15,000$ K. The spectra show much narrower Ly-α absorption as one moves away from this position; e.g., looking along a sightline to a bright cluster 1″ to the SE, the H I column must be at least ten times smaller (with the exact amount depending upon the assumed age/temperature of the underlying population).

van Zee et al. (1998) produced high spatial resolution (5″) maps of the H I distribution in I Zw 18, using the Very Large Array (VLA), and found that the column density peaks in the SE half of the galaxy at 3×10^{21} atoms cm^{-2}. Because each of the two starbursting regions (NW and SE) subtends $\sim 3''$ on the sky, a sharp peak in the H I distribution would be much smaller than a VLA resolution element, and thus the column density could peak at a significantly larger value than the peak in the van Zee et al. (1998) map.

3.3. *Summary*

We have presented high spatial resolution images and spectra of the starburst galaxy I Zw 18. These spectra show strong WR/WC emission features originating in two compact clusters. From the He II λ1640 emission, we estimate that 6 WR/WC stars reside in a very UV-bright cluster situated well within the NW starbursting region, and that 5 WR/WC stars lie in a somewhat fainter cluster just outside of this region. The fact that any WR/WC stars exist at all in I Zw 18 is surprising, because canonical theory for the evolution of single, massive, non-rotating stars predicts few WR stars and no WC stars to form at the low metallicity of I Zw 18 (Meynet 1995; Cerviño & Mas-Hesse 1994).

The existence of WR/WC stars at the low metallicity of I Zw 18 demonstrates the importance of sophisticated models of massive star evolution. Maeder & Meynet (2001) find that the inclusion of rotation in their models decreases the minimum mass for a single star to become a WR star, allowing the formation of WR stars at lower metallicity. Furthermore, there is both theoretical and observational evidence for the importance of close binary evolution in the formation of WR stars, especially as one moves to lower metallicity (see Bartzakos, Moffat, & Niemela 2001); the role of binaries in WR formation has a long history (see Paczyński 1967), even though much of the WR literature focuses on single-star evolution.

Our data also show a sharp peak in the H I column density of I Zw 18, situated within the SE half of the galaxy. This peak falls within the peak of previous high spatial resolution maps of the H I taken with the VLA (van Zee et al. 1998). However, our measurement of 2×10^{22} atoms cm^{-2} exceeds the earlier estimates by an order of magnitude, because of the higher resolution in our HST data.

Support for proposal 9054 was provided by NASA through a grant from the Space Telescope Science Institute, which is operated by the Association of Universities for Research in Astronomy, Inc., under NASA contract NAS 5-26555. The authors are grateful to C. Leitherer for advice and useful discussions. A. Aloisi kindly provided her catalog of WFPC2 photometry.

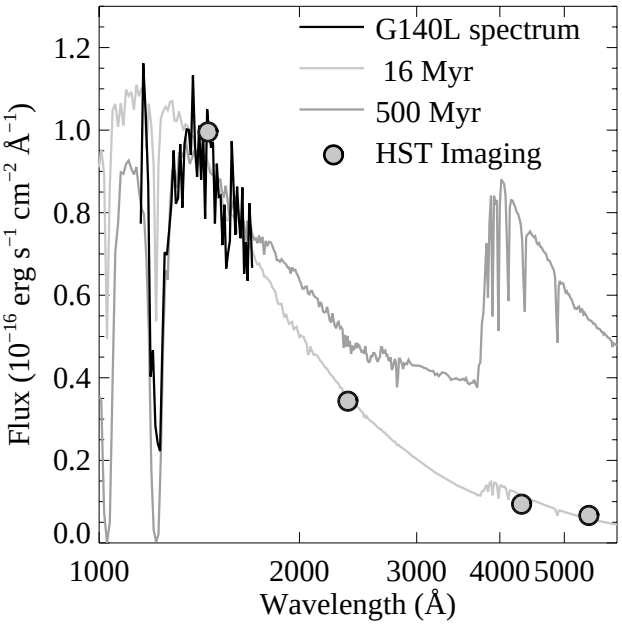

FIG. 2– Our spectrum showing the broadest Ly-α absorption (see Figure 1*a*), here over a longer wavelength baseline, combining the G140L data (black curve) and HST images (circles). The flux decline at longer wavelengths and the small Balmer jump show clearly that this region is dominated by a population of hot stars. To demonstrate, we show the integrated flux from a lightly reddened 16 Myr population (dark grey curve) and the flux from an unreddened 500 Myr population (light grey curve). An H I column of 2×10^{22} atoms cm^{-2} is required (not shown for clarity) to produce the width of the Ly-α absorption if a young (hot) population of stars is assumed.

REFERENCES

Aloisi, A., Tosi, M., & Greggio, L. 1999, AJ, 118, 302
Bartzakos, P., Moffat, A.F.J., & Niemela, V.S. 2001, MNRAS, 324, 18
Bertelli, G., Bressan, A., Chiosi, C., Fagotto, F., & Nasi, E. 1994, A&AS, 106, 275
Cannon, J.M., Skillman, E.D., Garnett, D.R., & Dufour, R.J. 2002, ApJ, 565, 931
Cerviño, M., & Mas-Hesse, J.M. 1994, A&A, 284, 749
de Mello, D.F., Schaerer, D., Heldmann, J., & Leitherer, C. 1998, ApJ, 507, 199
Dufour, R.J., Garnet, D.R., Skillman, E.D., & Shields, G.A. 1996, in From Stars to Galaxies, ed. C. Leitherer, U.Fritze-v. Alvensleben, & J. Huchra (San Francisco: ASP), 358
Gräfener, G., Koesterke, L., & Hamann, W.-R. 2002, A&A, 387, 244
Hunter, D.A., & Thronson, H.A., Jr. 1995, ApJ, 452, 238
Izotov, Y.I., Foltz, C.B., Green, R.F., Guseva, N.G., & Thuan, T.X. 1997, ApJ, 487, L37
Kimble, R.A., et al. 1998, ApJ, 492, 83
Kurucz, R.L. 1993, CD-ROM 13, ATLAS9 Stellar Atmosphere Programs and 2 km/s Grid (Cambridge: Smithsonian Astroph. Obs.)
Legrand, F., Kunth, D., Roy, J.-R., Mas-Hesse, J.M., & Walsh, J.R. 1997, A&A, 326, L17
Maeder, A., & Meynet, G. 1994, A&A, 287, 803
Maeder, A., & Meynet, G. 2001, A&A, 373, 555
Meynet, G. 1995, A&A, 298, 767
Niedzielski, A., & Rochowicz, K. 1994, A&AS, 108, 669
Östlin, G. 2000, ApJ, 535, L99
Paczyński, B. 1967, AcA, 17, 355
Schaerer, D., & Vacca, W.D. 1998, ApJ, 497, 618
Schlegel, D.J., Finkbeiner, D.P., & Davis, M. 1998, ApJ, 500, 525
Stetson, P.B. 1987, PASP, 99, 191
Thuan, T.X., Lipovetsky, V.A., Martin, J.-M., & Pustilnik, S.A. 1999, A&AS, 139, 1
Vílchez, J.M., & Iglesias-Páramo, J.L. 1998, AJ, 115, 1000
van Zee, L., Westpfahl, D., Haynes, M.P., & Salzer, J.J. 1998, AJ, 115, 1000

Witt, A.N. & Gordon, K.D. 2000, ApJ, 528, 799
Woodgate, B.E., et al. 1998, PASP, 110, 1183